

## 49. GEOCHEMISTRY AND ORIGIN OF EAST PACIFIC SEDIMENTS SAMPLED DURING DSDP LEG 34

Kurt Boström,<sup>1</sup> Oiva Joensuu, Sylvia Valdés, Wally Charm, and Robert Glaccum,  
Rosenstiel School of Marine and Atmospheric Science, University of Miami, Miami, Florida

### INTRODUCTION

Several papers have recently appeared about the metalliferous sediments on the active (spreading) oceanic ridges. The geochemistry and mineralogy of such sediments are now reasonably well known, and generally these deposits are considered to be products of volcanic processes. The nature of this volcanism is still unclear: both deep-seated volcanic centers (Arrhenius and Bonatti, 1965; Boström and Peterson, 1966) and shallow hydrothermal leaching of basalts (Boström, 1967; Corliss, 1971) have been discussed as possible sources for the metal-rich sediments. However, such hydrothermal leaching is probably an insufficient process since it neither accounts for the observed accumulation rates for iron and manganese, nor for the observed Fe/Al and Fe/Ti ratios in the sediments (Boström, 1973; in press). Biological sources possibly account for some traces, (e.g., Ba and Cu, Turekian, 1968; Boström et al., 1974b; Moore et al., in preparation), but to what extent is not known. The need for further studies of active ridge deposits is therefore great, particularly in view of the significance such deposits may have as sources for primary or secondary enrichment of Fe, Mn, Cu, etc. in various economic deposits (Sillitoe, 1972; Boström et al., 1972b; Boström, 1973). The sampling by *Glomar Challenger* in an area with well-developed active ridge deposits was therefore of utmost importance for a discussion of how active ridge deposits originate.

### EXPERIMENTAL METHODS AND RESULTS

The material for this study (about 150 samples) was collected by one of us (Charm) on board *Glomar Challenger*. The procurement of material immediately after the recovery of the sediment cores considerably decreased the risk of contamination, which may affect samples after long storage. The samples were never taken close to the core liner or the surface of splitting in order to lessen the risk for contamination. The strong resemblance between the analytical results presented here and in many other publications (Boström et al., 1972b; Boström, 1973) suggests that the contamination is negligible in most studies in the past as well as in this study.

After being transferred to the University of Miami, 95 samples were selected for analysis, which were dried, ground, and subsequently split into fractions. One fraction was analyzed by atomic absorption spectrophotometry (S.V.) for NaCl, CaCO<sub>3</sub>, Si, Al, Fe, Mn, P,

Cu, Zn, Mg, and Sr (of which the two last elements are not further discussed in this paper). Another fraction was analyzed by emission spectrometry (O.J.) for Si, Ti, Fe, Mn, P, B, Ba, Cu, Co, Ni, La, Sc, Y, Cr, V, and Zr. Procedures and analytical accuracies are similar to those reported in Boström and Peterson, 1969; Boström et al., 1972b.

The distribution of the samples and the original values are given in Tables 1 and 2. Table 3 presents a grouping of the material into chronological units, for which accumulation rates can be calculated. Tables 4 to 8 and Figures 1 to 4 present additional material that will be discussed in the following. In this paper the chemistry of concretionary matter, oxide coatings on rocks, etc. have been disregarded, since their total masses and rates of accumulation are small compared to other deep-sea sediments.

### SEDIMENT-PETROGRAPHIC NORM CALCULATIONS

Norm calculations have played a large role in the study of igneous rocks, but have been used infrequently by sedimentologists. The motivation for norm calculations is that "rock analyses can be quantitatively studied and compared from a petrological point of view" (Barth, 1952).

In this paper, extensive use is made of such calculations. As was pointed out in Boström et al. (1972b), recalculation on a carbonate-free basis is a poor procedure, particularly when the carbonate content is high; then even small fluctuations (that is, errors) in CaCO<sub>3</sub> content will lead to sharp fluctuations in the carbonate-free basis values. This can be corrected if very careful analyses are produced for the carbonate, total interstitial salt, organic matter, and total water content. Unfortunately, this procedure involves much work and is expensive and time consuming. A simpler procedure is to recalculate the sum of the major oxides, sulfates, etc., to a given sum as is outlined in the note for Table 5; by this method even the diluting effect by opaline silica can be removed.

We do not claim that these procedures represent the final end product; certainly many improvements can be added. Yet these norms, as well as the element ratios presented in Figures 1, 2, and 3 do give a clearer picture of the compositional relationships in deep-sea sediments than do the unprocessed data in Tables 2 or 4.

### DISCUSSION

#### Chemical Analyses

The results reported in Table 2 show striking similarities with data already published elsewhere. As in

<sup>1</sup>Present address: Department of Economic Geology, University of Lulea, 951 87, Sweden.

TABLE 1  
Sample Distribution

Sample No.	DSDP Sample (Interval in cm)	Age	Note
<b>Hole 319</b>			
1	1-1, 98.5-100.5	Quat.	
2	1-2, 148-150		
3	1-3, 0-10		
4	1-3, 0-10		IWS
5	1-4, 146-148		
6	1-5, 0-10		
7	1-5, 0-10	Late Miocene to Pliocene	IWS
8	1-5, 99-101		
9	2-2, 95-97		
10	2-3, 0-10		
11	2-3, 0-10		IWS
12	3-2, 89-91		
13	3-3, 0-10		
14	3-3, 0-10		IWS
15	4-3, 64-66		
16	5-6, 0-10		
17	5-6, 0-10		IWS
18	7-4, 3-5		
19	7-5, 144-150		
20	7-5, 144-150		IWS
21	8-5, 84-86	Middle Miocene	
22	9-2, 122-124		
23	9-2, 140-150		
24	9-2, 140-150		IWS
25	9-3, 98-100		
26	10-2, 120-122		
27	10-5, 36-38		
28	11-2, 100-102		
29	11-2, 142-150		
30	11-2, 142-150		IWS
31	11-3, 136-138		
32	11-5, 10-12		
33	11-5, 142-150		
34	11-5, 142-150		IWS
35	11-6, 14-16		
36	12-2, 10-12		
37	12-2, 50-52		
38	12-2, 90-92	Early Miocene	
39	12-2, 130-132		
40	12-3, 0-7		
41	12-3, 0-7		IWS
42	12-3, 5-7		
43	12-3, 25-27		
44	12-3, 63-65		
45	12-3, 95-97		
46	12-3, 115-117		
47	12-3, 125-127		
48	12-3, 143-145		
<b>Hole 320</b>			
49	1-1, 20-22		
50	1-1, 36-39		
51	1-1, 62-64		
52	1-2, 68-70	Quat.	
53	1-4, 57-59		
54	1-6, 71-73		
55	1-2, 144-150		IWS
56	1-5, 144-150		IWS
57	2-2, 99-101		
58	3-2, 136-138	Early Miocene	
59	3-2, 144-150		IWS
60	3-4, 74-76		
61	3-6, 122-124		

TABLE 1 - Continued

Sample No.	DSDP Sample (Interval in cm)	Age	Note
<b>Hole 320B</b>			
62	1-1, 129-131		
63	1-3, 138-140		
64	1-5, 122-124	Late Oligocene to early Miocene	IWS
65	1-5, 143-150		
66	2-1, 86-88		
67	2-3, 111-113		
68	2-5, 132-134		
69	2-5, 140-150		IWS
<b>Site 321</b>			
70	2-2, 56-58		
71	2-4, 0-6		IWS
72	3-2, 101-102	Quat.	
73	4-2, 56-58		
74	4-3, 144-150		IWS
75	5-4, 138-140	Pliocene-Pleistocene	
76	6-2, 106-108		
77	6-4, 130-132	Late Miocene	IWS
78	6-4, 144-150		
79	6-6, 142-144		
80	7-2, 138-140		
81	7-4, 139-141	Late Oligocene to early Miocene	IWS
82	7-6, 125-127		
83	8-1, 135-137		
84	9-1, 15-17		
85	9-5, 31-33		
86	9-6, 0-6		IWS
87	10-2, 120-122	Middle Oligocene	
88	11-2, 90-92	Early Oligocene	IWS
89	11-4, 0-6		
90	13-1, 145-147		
91	13-3, 0-6		IWS
92	13-3, 42-44	Late Eocene	
93	13-3, 82-84		
94	13-3, 102-104		
95	13-3, 122-124		

<sup>a</sup>IWS = Samples that have been squeezed for interstitial water studies.

the DSDP crossing in the South Atlantic (Leg 3, Boström et al. 1972b), there is a pronounced tendency for the Fe-, Mn-, V-rich and Si-, Al-, Ti-poor sediments to occur in the basal layer of the sediments. Thus, all sediments that are rich in Fe, Mn, P<sub>2</sub>O<sub>5</sub>, and V, or show high accumulation rates for these constituents, were formed within 20 m.y. from the generation of their basaltic substratum (groups A, B, C, D, F, G, K, L, M, and N). This is the distribution pattern one would expect if ferromanganoan sediments are the first to form at spreading centers (Boström and Peterson, 1969) and confirms the validity of this interpretation. There is now little doubt that such sediments exclusively originate on active ridges, partly involving some form of submarine volcanism. The data in Figures 1 and 2 suggest that the volcanic source delivers material of remarkably constant composition; otherwise, a much larger scatter should be expected in the petrochemical graphs. The same graphs also clearly demonstrate that the only other phase of

significance that involves Fe, Mn, Al, and Ti is terrigenous material (TM as defined in Table 8); most remarkable is the negligible significance of lithogenic matter of basaltic origin. (See also Boström et al., 1973b.)

#### Accumulation Rates

The data in Tables 3 and 4 have been used to calculate the accumulation rates presented in Table 6. The data show that the highest accumulation rates of authigenic Fe-Mn phases occur close to spreading centers, that is, in the basal sediments. Similar patterns are found for B, Cu, Ni, V, P, and Zn whereas the pattern is opposite for Al and Ti. Less clear are the patterns for Co, Y, Zr, SiO<sub>2</sub>\*, and Ba (for which nevertheless some of the high Ba accumulation rates are found in sediments with high accumulation rates for Fe and Mn). There are, however, problems with these calculated accumulation rates. Uncertainties in dating and in physical properties of the sediments may give errors on the order of 10%-20% in the values presented. More serious are the errors that may be physiographically induced; the topography of the ocean floor may enhance or lessen the observed accumulation rates due to slumping, turbidite flows, or gentle winnowing of matter (van Andel et al., 1967). Bottom currents obviously intensify the disturbing processes. As a result of such processes, undisturbed cores suitable for dating and accumulation rate studies are difficult to obtain on the Mid-Atlantic Ridge (MAR). The sediment distribution on the East Pacific Rise (EPR), on the other hand, is different. Thus, the EPR is characterized by a very smooth and gentle topography and only close to the spreading center does bare rock make up considerably more than 50% of the area (Boström et al., 1974a). Because of this fact, extensive coring was performed on or close to the crest of the EPR at about 14°-15°S and several 8-9 meter long sediment cores were procured, even on topographic elevations during cruise GS 7202 of the University of Miami (Spring 1972). Most remarkable was an 8.5-meter long core (GS 7202-35 P) recovered from a hilltop only 80 km west of the spreading center. Studies of this core suggest essentially undisturbed sedimentation for at least the last 600,000 years; the only disturbance of any significance may have been a slight loss of fines from the hilltop due to down-slope winnowing (Boström et al., 1974a). The accumulation rates for core GS7202-35 P presented in Table 6 may therefore be too low, but show good order-of-magnitude agreement with accumulation rates for groups C and D.

The accumulation rates for the sediments at Site 319 may nevertheless be somewhat high. Studies of PDR records at University of Miami and at Scripps Institution of Oceanography, as well as coring results, suggest that about 70% of the present Bauer Deep is sediment covered (Boström et al., 1973a) and airgun profiles suggest that the older sediments cover about 30%-35%. This implies that observed accumulation rates, at least for the lower part of Hole 319, may be about twice as large as undisturbed, evenly distributed accumulation would give. Similar comments may pertain to the lowest parts of Hole 320 and Site 321. However, the difficulties

in correctly assessing the influence of the "paleotopography" when the basal sediments were deposited at Hole 320 and Site 321 makes it difficult to know with certainty whether the accumulation rates in the basal layers may be too low or too high. Nevertheless, the remarkable similarities in chemistry and overall accumulation rates for many constituents in the basal sediments in Holes 319-321 with recently forming deposits on the EPR strongly suggest that the rapid formation of Fe-Mn-rich, Al-Ti-poor sediments has been a nearly continuous process at the East Pacific spreading centers (either on the EPR or on the Galapagos Rise) for the last 36 m.y. This is particularly well emphasized with the normalized values presented in Table 5.

#### Relationships Between Spreading Rates and the Chemistry of the Sediments

Previous studies show that there is a distinct relationship between the composition of basal sediments and the spreading rates at the plate-generating zone, (see Figure 3 and Boström, 1973).

The relationship  $(\text{Fe} + \text{Mn})/\text{Al}$  can be written as an exponential function of the spreading rate as follows:

$$\frac{\text{Fe} + \text{Mn}}{\text{Al}} = 0.59 \times e^{0.53\text{SR}}$$

where SR = spreading rate in cm/year.

This relationship indicates that exhalations at centers with rapid spreading surface rapidly implying that the rate of admixture of terrigenous, basaltic, and biogenic matter must be outpaced, which accounts for the variations in the ratio  $(\text{Fe} + \text{Mn})/\text{Al}$ . Such variations cannot be deduced from the data in Figure 1 alone. This spreading-rate dependence for Fe and Mn strongly suggests an intimate connection with those volcanic processes that are associated with the rate of generation of new basaltic crust, that is, possibly with the splitting of pyrolite into residual peridotite, basalt, and a minor quantity of exhalations. For the basal sediments from Holes 319-321 this  $(\text{Fe} + \text{Mn})/\text{Al}$  ratio varies between 15 and 23. According to the best-fit curve, this would correspond to a spreading rate of 6.0-6.7 cm/year (see Figure 3), which is very close to the spreading rates of 6-7 cm/year for those sites where Holes 319, 320, and 321 are located. Hole 319 is associated with a segment of the EPR that has spreading rates of about 6-7 cm/year according to Herron (1972). Hole 320 and Site 321 are located approximately 1700 km from the old Galapagos spreading center and were displaced by spreading from about 35 m.y. B.P. (age of the basal sediment) until 10 m.y. B.P., at which time the Galapagos Ridge ceased to be active (Hays et al., 1972). This implies that spreading took place at a little less than 7 cm/year.

#### Origin of Major Constituents in the Basal Sediments

The well-defined main element composition of the active ridge-derived matter (see Figures 1 and 2) and the relationship between spreading rates and  $(\text{Fe} + \text{Mn})/\text{Al}$  values point to an origin related to the same process that controls the spreading rate. A possible interpretation is

TABLE 2  
Original Analytical Results for Sediment Samples Obtained During DSDP Leg 34

Sample No.	Na (%)	SiO <sub>2</sub> (%)	Ti (%)	Al (%)	Fe (%)	Mn (%)	P <sub>2</sub> O <sub>5</sub> (%)	B (ppm)	Ba (ppm)	Co (ppm)	Cr (ppm)	Cu (ppm)	La (ppm)	Ni (ppm)	Sc (ppm)	V (ppm)	Y (ppm)	Zr (ppm)	Zn (ppm)
1	5.3	29	0.16	2.5	13.3	3.99	2.1	150	9100	220	13	850	280	540	17	190	1200	720	795
2	4.7	29	0.32	2.2	14.1	3.30	1.7	170	9700	180	8	890	230	540	16	220	620	310	340
3, 4	4.7	30.5	0.24	2.4	14.6	3.45	1.8	165	12500	175	11	910	200	540	14	230	555	240	347
5	3.1	18	0.090	2.3	14.7	3.57	1.5	160	8000	140	10	890	190	360	8.5	270	360	250	330
6, 7	1.7	17.2	0.076	1.2	15.6	3.54	1.4	130	7400	135	6	880	150	250	8.2	290	290	210	325
8	0.89	11.7	0.030	0.47	6.3	1.47	0.61	60	3900	52	< 10	390	35	140	NA	130	120	70	175
9	0.45	12.0	0.022	0.25	5.7	0.89	0.32	45	3300	24	< 10	320	9	90	NA	60	60	48	120
10, 11	0.85	11.6	0.024	0.28	5.1	1.09	0.29	46	3000	22	~ 2	330	27	85	~ 2.0	75	57	52	175
12	0.82	14.3	NA	0.38	6.9	1.24	0.45	NA	NA	NA	NA	NA	NA	NA	NA	NA	NA	NA	NA
13, 14	1.4	16.8	0.028	0.47	7.8	1.55	0.55	72	3600	19	< 5	510	45	115	3.5	135	115	100	180
15	0.82	2.3	0.0070	0.16	2.7	0.56	0.25	50	1200	7	< 5	160	42	42	< 2	85	42	32	145
16, 17	0.50	0.63	0.0015	0.040	0.67	0.15	0.12	30	360	~ 5	< 5	57	< 10	10	< 2	10	12	9	43
18	0.74	1.3	0.0030	0.11	1.2	0.29	0.16	37	720	7	< 5	94	< 10	15	4	23	22	16	160
19, 20	0.60	1.0	0.0022	0.075	0.85	0.21	0.12	48	780	5.7	< 5	68	< 10	15	4	17	16	11	42
21	0.78	1.9	0.013	0.15	2.0	0.56	0.25	64	NA	19	< 5	180	25	42	8	90	36	32	77
22	0.80	2.8	0.016	0.23	5.0	2.17	0.37	70	1050	27	< 5	350	33	150	7	210	42	45	170
23, 24	0.66	1.7	0.010	0.15	2.9	1.80	0.30	50	1350	20	< 5	200	21	100	< 2	125	28	28	100
25	1.26	3.6	0.019	0.29	5.2	2.55	0.43	70	1020	32	< 5	430	33	200	2.5	230	44	48	210
26	0.74	1.1	0.0078	0.080	2.0	0.60	0.20	45	560	18	< 5	120	< 10	60	< 2	75	22	22	70
27	0.74	1.0	0.0084	0.11	1.9	0.62	0.18	30	720	19	< 5	135	< 10	60	< 2	75	16	20	83
28	0.73	1.2	0.0096	0.080	2.4	1.00	0.25	42	660	42	< 5	165	< 10	90	< 2	100	26	26	96
29, 30	0.56	1.0	0.0069	0.095	1.9	0.70	0.24	39	515	8	< 5	125	NA	67	~ 2	80	16	17	80
31	0.91	2.7	0.017	0.21	5.2	2.17	0.40	65	1100	30	< 5	320	30	180	6.5	190	30	40	175
32	0.49	1.6	0.0078	0.13	3.0	0.17	0.27	50	620	18	< 5	150	12	70	3.5	85	16	20	85
33, 34	0.64	1.4	0.0078	0.12	2.2	0.70	0.24	47	810	14	< 5	130	~ 6	40	3.0	64	16	16	70
35	0.70	2.1	0.0102	0.16	4.4	1.29	0.34	60	1100	17	< 5	155	13	110	3.5	95	21	22	110
36	0.62	1.9	0.0084	0.16	2.2	0.62	0.27	40	380	18	< 5	135	14	53	4.5	60	16	20	69
37	0.61	1.7	0.0078	0.15	1.5	0.41	0.25	37	830	11	< 5	80	< 10	35	< 2	30	30	13	39
38	0.59	1.6	0.0072	0.16	1.2	0.33	0.25	35	820	8	< 5	85	< 10	19	< 2	24	24	13	62
39	0.55	1.6	0.0066	0.11	0.85	0.21	0.22	45	850	7	< 5	55	< 10	17	< 2	16	16	13	41
40, 41	0.37	1.2	0.0063	0.11	0.93	0.23	0.20	32	760	7	< 5	55	< 10	17	< 2	15	12	12	37
42	0.58	1.3	0.0072	0.11	1.0	0.23	0.21	35	710	11	< 5	55	< 10	20	< 2	18	12	13	42
43	0.50	1.1	0.0060	0.080	0.75	0.19	0.21	35	730	6.5	< 5	45	< 10	17	< 2	17	12	12	41
44	0.52	1.3	0.0072	0.10	0.95	0.25	0.24	55	650	14	< 5	60	< 10	21	< 2	22	19	25	42
45	0.86	6.0	0.021	0.28	4.2	1.11	0.33	65	1450	16	< 5	85	< 10	95	< 2	90	24	40	120
46	0.56	1.7	0.016	0.13	1.5	0.40	0.28	37	720	14	< 5	120	< 10	37	< 2	41	16	17	58
47	0.65	2.4	0.013	0.21	2.6	0.88	0.32	70	780	19	< 5	135	< 10	27	< 2	75	22	20	81
48	0.59	3.4	0.0078	0.13	2.7	0.61	0.31	40	1200	12	< 5	140	< 10	50	< 2	55	15	17	70
49	3.12	54	0.34	10.21	4.3	0.081	0.14	130	3300	17	95	190	25	160	16	195	22	122	330
50	3.71	48	0.34	10.21	4.2	0.620	0.18	95	3900	20	75	290	28	180	14	190	26	122	250
51	3.71	52	0.38	7.94	4.3	0.081	0.14	110	2700	22	86	240	30	240	18	270	22	120	330
52	4.10	52	0.37	5.93	3.4	0.121	0.12	105	2900	14	47	360	30	240	14	220	20	100	390
53	3.49	50	0.32	6.46	5.8	0.089	0.11	115	3100	24	59	220	25	320	14	200	17	110	250
54	3.26	50	0.32	7.41	4.2	0.124	0.21	115	3300	14	95	240	28	190	14	165	31	120	310
55	2.60	53	0.39	8.2	4.4	0.074	0.18	110	4400	13	97	260	25	180	16	260	27	130	360
56	2.23	52	0.32	6.9	4.2	0.14	0.13	130	3100	15	75	210	35	240	18	210	22	125	350
57	2.60	23	0.084	1.6	8.9	2.6	0.47	90	4100	34	10	590	15	130	4	190	22	110	280
58	0.74	2.9	0.0054	0.090	1.9	0.56	0.12	45	760	8	< 10	90	< 10	34	< 3	42	13	17	70
59	0.37	2.2	0.0036	0.090	1.9	0.58	0.11	40	600	7	< 10	82	< 10	41	< 3	39	12	18	70
60	0.70	2.2	0.0030	0.074	1.5	0.41	0.092	42	650	8	< 10	80	< 10	30	< 3	26	13	14	40
61	0.70	1.8	0.0033	0.079	1.5	0.43	0.092	45	650	9	< 10	70	< 10	32	< 3	26	13	13	60
62	0.82	3.3	0.0078	0.12	1.6	0.50	0.11	90	730	10	< 10	105	< 10	51	< 3	27	14	16	50
63	0.65	2.4	0.0072	0.095	1.5	0.31	0.10	35	810	7	< 10	75	< 10	33	< 3	57	7	16	40
64	0.70	6.1	0.010	0.18	2.6	0.85	0.12	46	580	11	< 10	130	< 10	72	< 3	75	11	20	80
65	0.46	4.1	0.011	0.14	2.2	0.96	0.14	48	810	8	28	160	< 10	80	< 3	85	12	20	80
66	0.78	2.9	0.011	0.14	2.0	0.76	0.19	40	600	7	< 10	77	< 10	42	< 3	80	8	20	70

TABLE 2 – Continued

Sample No.	Na (%)	SiO <sub>2</sub> (%)	Ti (%)	Al (%)	Fe (%)	Mn (%)	P <sub>2</sub> O <sub>5</sub> (%)	B (ppm)	Ba (ppm)	Co (ppm)	Cr (ppm)	Cu (ppm)	La (ppm)	Ni (ppm)	Sc (ppm)	V (ppm)	Y (ppm)	Zr (ppm)	Zn (ppm)
67	0.67	2.9	0.078	0.11	2.0	0.79	0.17	100	650	7	< 10	135	< 10	75	< 3	80	8	18	60
68	0.63	2.2	0.011	0.11	3.0	0.91	0.22	45	610	11	< 10	160	< 10	68	< 3	110	13	20	60
69	0.41	3.3	0.0090	0.10	1.6	0.70	0.18	48	810	7	< 10	89	< 10	53	< 3	70	9	22	50
70	3.71	52	0.30	8.0	4.9	0.051	0.18	105	3400	24	86	210	32	130	17	160	45	160	180
71	2.37	57	0.53	7.7	5.2	0.053	0.21	105	3700	22	78	290	30	68	17	210	45	190	160
72	3.71	54	0.35	7.4	4.7	0.050	0.17	105	3400	36	77	280	52	120	16	180	40	160	160
73	4.23	54	0.31	7.2	4.7	0.093	0.14	110	3400	110	90	1300	54	330	18	190	40	170	270
74	2.40	52	0.34	7.5	5.2	0.071	0.21	110	4100	52	105	590	53	260	22	155	52	175	220
75	3.71	55	0.35	6.8	4.8	0.10	0.24	110	4900	52	88	590	60	340	16	105	70	175	210
76	4.30	48	0.29	6.4	4.8	0.37	0.39	90	4600	47	90	510	52	300	12	100	77	150	230
77	4.45	52	0.31	5.9	6.0	0.25	0.35	110	1100	45	120	530	60	370	17	100	69	190	260
78	3.71	45	0.32	6.1	6.4	0.19	0.39	100	8200	50	115	610	82	440	36	110	86	170	280
79	3.71	51	0.30	6.1	6.1	0.71	0.36	105	5200	130	90	640	85	440	14	100	88	175	190
80	3.93	51	0.28	6.4	6.6	2.2	0.99	110	7600	180	25	720	170	390	29	110	230	200	270
81	3.00	50	0.33	6.6	7.7	3.1	1.38	110	4100	320	31	690	190	460	36	190	280	260	240
82	2.23	36	0.30	4.3	13.7	4.2	2.0	140	1900	190	27	830	210	620	26	170	240	220	450
83	0.60	1.5	0.0084	0.19	0.41	0.12	0.089	55	240	< 5	< 10	290	< 10	19	< 3	6	8	14	70
84	2.08	24	0.17	3.7	7.8	1.9	1.06	92	760	140	27	510	85	270	11	200	170	180	230
85	1.14	8.2	0.060	1.3	7.8	1.4	0.62	90	360	48	16	440	ND	160	4	390	80	95	240
86	0.76	5.2	0.066	1.5	9.6	1.9	0.74	80	330	75	11	410	65	260	7	220	40	110	270
87	0.73	1.9	0.0090	0.22	1.3	0.31	0.16	82	120	7.5	< 10	50	< 10	22	< 3	27	17	25	50
88	0.56	1.8	0.0078	0.19	0.77	0.20	0.11	40	220	4	< 10	35	< 10	14	< 3	13	12	17	40
89	0.32	2.0	0.0096	0.22	0.92	0.25	0.14	30	370	4	< 10	32	< 10	13	< 3	14	30	22	40
90	0.70	3.9	0.037	0.40	4.6	2.6	0.29	45	550	13	< 10	320	ND	180	< 3	170	55	45	190
91	0.50	2.6	0.022	0.26	5.4	2.8	0.29	60	340	22	< 10	260	ND	240	< 3	170	28	35	180
92	0.95	2.7	0.051	0.28	4.7	2.3	0.27	60	310	13	< 10	240	ND	160	< 3	170	19	35	160
93	0.82	3.5	0.057	0.30	4.4	2.0	0.29	110	330	17	10	260	ND	190	3	190	20	30	140
94	1.00	6.5	0.096	0.51	3.7	1.4	0.26	60	300	17	10	180	ND	140	4	160	15	29	110
95	1.30	15.5	0.22	1.01	5.0	1.6	0.18	80	420	28	15	180	ND	170	5	130	16	28	140

Note: All values are given on an absolute basis in wt % or weight ppm for samples dried at 100°C; that is, no correction for carbonate content has been made. NA = not analyzed (for instance, due to loss of samples). ND = not determined (for instance, due to severe interference from other spectral lines). Values given for double samples (for instance, 3&4, 6&7, 10&11, etc) represent averages of two analyses of two aliquots of the same sampling spot in the section.

TABLE 3  
Sample Distribution, Physical Properties, Geochronology, and Accumulation Rates  
for Sediments Sampled During DSDP Leg 34

Group	Core Section	DISUD (g/CC)	Layer Below Mud line (m)	Thickness (m)	Age (m.y.)	Sedimentation Rate (mm/1000 yr)	Accumulation Rate of Sediment (mg/cm <sup>2</sup> 1000 yr)
<b>Hole 319</b>							
A (1)	1-1	0.33	0-2	2	0-2	1.0	33
B (13)	1-2 to 3-3	0.41	2-23	21	2-12	2.0	86
C (13)	3-3 to 10	1.01	23-95	72	12-14	36	3600
D (21)	11 and 12	1.10	95-111.5	16.5	14-15	16.5	1800
<b>Hole 320</b>							
E (8)	1	0.41	0-16	16	0-2	8	330
F (5)	2 and 3	0.97	>(74-112)	>38	15-20	> 7.6	> 740
G (8)	1B and 2B	1.11	>(136-155)	>19	22-30	> 2.4	> 270
<b>Site 321</b>							
H (5)	1 to 4	0.36	0-30	30	0-2	15	540
I (1)	5	0.76	30-39.5	9.5	2-2.5	2.7	210
J (4)	6	0.71	39.5-49	9.5	5.5-12	1.5	110
K (7)	7 to 9	0.86	49-77.5	28.5	22-35	2.2	190
L (1)	10	1.20	77.5-87	9.5	35-36.5	6.3	760
M (2)	11, 12	1.10	87-115.5	28.5	36.5-38	19.0	2090
N (6)	13	1.02	115.5-125	9.5	38-41	3.2	330

Note: Data in this table are based on chronological information (primarily foraminifera zones), bulk densities, porosities, and depth distribution of the samples that have been presented elsewhere in this volume and in Table 1. Furthermore, absolute sedimentation rates were obtained using the relationships between relative and absolute ages (Berggren, 1969; and later revisions). Number in parentheses behind each group label (A, B, etc) represents number of analyses used for the averaging in Tables 4 to 6. DISUD stands for dry in situ uncompressed density, in other words, the weight of the dry matter within a cc at the sampling depth. DISUD is easily calculated from the bulk densities and porosities presented elsewhere in this volume. Note that the incomplete coring of Hole 320 gives rise to very uncertain data for groups F and G. Other uncertainties, for instance, whether groups L and M should be presented as a single group or separately, are caused by ambiguities in chronological descriptions. However, a combined group (L + M) would have an accumulation rate of about 1700 mg/cm<sup>2</sup>1000 yr; the overall accumulation rate patterns presented in this paper will therefore not change if L and M were combined. Group M may be particularly overestimated due to these uncertainties, but a study of Table 6 reveals that even if the accumulation rate data for M are reduced with 50%, this does not alter the overall conclusions in this paper. Likewise, data for group N might be somewhat underestimated; if corresponding "correction" is included in Table 6 the conclusions in this paper are even more reinforced. It is therefore obvious that minor uncertainties in the accumulation rate data do not significantly affect the results in this paper, but they are serious enough to prevent a far-reaching in detail discussion of what has happened with the sediments, as is clearly demonstrated in the section of the paper that discusses paleogeographic problems.

that with increased spreading rates more intense heat flow also takes place through the ocean floor. The higher heat flow should result in stronger hydrothermal leaching than is possible in areas of low heat flow. However, studies of hot springs in basaltic areas suggest that there is no significant differentiation between Fe and Al, that is, the formed solutions contain equal quantities of Al and Fe. The same conclusion is obtained from experimental leaching experiments involving basaltic matter and weak to strong NaCl brines; also, there is no significant segregation of the elements Fe, Mn, Al, and Ti during the magmatic or effusive phases that emplace basalt in shallow regions of the oceanic crust. Furthermore, it does not appear likely that spilitization of lavas would give rise to Fe-Mn-rich, Al-Si-Ti-poor solutions. Carbonate-rich emanations, on the other hand, tend to be enriched in Fe, Mn, P, Ba, and U and depleted in Al, Ti, Si, and Th. It is, therefore, possible that carbonate-

rich emanations from the mantle may play a major role in the separation of these elements. Green (1972) has shown that much CO<sub>2</sub> may indeed emanate from the mantle. The problems discussed above in this section have been reviewed at length by Boström (1973).

The discussion here has referred to the major element distribution in the sediments. Data in Boström et al., 1973a, Boström, in press) give additional support to the conclusion that the influx of terrigenous matter and some addition of an EPR constituent (see Figures 1 and 2) control the main element composition of the sediments, whereas sources of basaltic detritus are less significant.

#### Origin of Trace Constituents in the Basal Sediments

The sources for the trace elements in the East Pacific sediments are less easily determined. For this discussion we will use data in Tables 7 and 8 and graphical displays

TABLE 4  
Average Chemical Compositions of Sediments Recovered During DSDP Leg 34

Group	SiO <sub>2</sub> (%)	Ti (%)	Al (%)	Fe (%)	Mn (%)	P <sub>2</sub> O <sub>5</sub> (%)	B (ppm)	Ba (ppm)	Co (ppm)	Cr (ppm)	Cu (ppm)	La (ppm)	Ni (ppm)	Sc (ppm)	V (ppm)	Y (ppm)	Zr (ppm)	Zn (ppm)
<b>Hole 319</b>																		
A	29	0.16	2.5	13.3	4.0	2.1	150	9100	220	13	850	280	540	17	190	1200	720	800
B	18	0.10	1.1	10.1	2.2	0.96	106	6400	93	~6	640	110	280	~7	175	270	160	250
C	1.7	0.0088	0.14	2.44	0.95	0.24	50	860	16	<5	180	~18	69	~3	94	28	26	110
D	2.0	0.0097	0.14	2.18	0.64	0.27	46	820	15	<5	116	<10	54	<2	60	19	20	73
<b>Hole 320</b>																		
E	51	0.35	7.9	4.35	0.17	0.15	114	3300	17	78	250	28	220	16	215	23	120	320
F	6.4	0.020	0.38	3.12	0.91	0.18	52	1350	13	<10	180	<10	53	<3	65	15	34	104
G	3.4	0.0093	0.12	2.06	0.72	0.15	57	700	8.5	<10	116	<10	59	<3	73	10	19	61
<b>Site 321</b>																		
H	54	0.37	7.6	4.93	0.064	0.18	107	3600	49	87	535	44	180	18	180	44	170	200
I	55	0.35	6.8	4.80	0.10	0.24	110	4900	52	88	590	60	340	16	105	70	175	210
J	49	0.31	6.1	5.81	0.38	0.37	100	4800	68	105	575	70	390	18	105	80	172	240
K	25	0.17	3.4	7.65	2.10	0.99	97	2200	137	20	555	120	310	16	185	150	155	255
L	1.9	0.0090	0.22	1.30	0.31	0.16	82	120	7.5	<10	50	<10	22	<3	27	17	25	50
M	1.9	0.0087	0.21	0.85	0.23	0.13	35	295	4	<10	34	<10	14	<3	14	21	20	40
N	5.8	0.081	0.46	4.63	2.1	0.26	69	375	18	~8.3	240	ND	180	~2.8	165	26	34	153

Note: All values are on an absolute basis; that is, no correction for CaCO<sub>3</sub>-content has been made. Much of the variations are due to the diluting effect of the CaCO<sub>3</sub> content. For definitions of groups A to N, see Table 3.

TABLE 5  
Compositions of Carbonate- and Opaline Silica-Free Fractions of Sediments Recovered During DSDP Leg 34

Group	Ti (%)	Al (%)	Fe (%)	Mn (%)	P <sub>2</sub> O <sub>5</sub> (%)	B (ppm)	Ba (ppm)	Co (ppm)	Cr (ppm)	Cu (ppm)	La (ppm)	Ni (ppm)	Sc (ppm)	V (ppm)	Y (ppm)	Zr (ppm)	Zn (ppm)
<b>Hole 319</b>																	
A	0.21	3.3	17.5	5.3	2.8	195	12,000	290	17	1100	370	710	22	250	1600	945	1050
B	0.23	2.4	22.0	4.8	2.1	230	14,000	200	~13	1400	240	610	~15	380	585	350	545
C	0.083	1.3	23.0	9.0	2.3	470	8,100	150	—	1700	~170	650	~28	885	265	245	1040
D	0.10	1.5	23.3	6.8	2.9	490	8,800	160	—	1240	—	575	—	640	205	215	780
<b>Hole 320</b>																	
E	0.38	8.6	4.71	0.18	0.16	125	3,600	18	84	270	30	240	17	235	27	130	345
F	0.14	2.6	21.2	6.2	1.2	355	9,200	88	—	1200	—	360	—	440	100	230	705
G	0.11	1.4	23.6	8.3	1.7	655	8,000	97	—	1300	—	675	—	835	115	220	700
<b>Hole 321</b>																	
H	0.41	8.4	5.43	0.071	0.20	120	4,000	54	96	590	48	200	20	200	48	185	220
I	0.42	8.2	5.79	0.12	0.29	135	5,900	63	105	710	72	410	19	125	84	210	255
J	0.35	6.8	6.51	0.43	0.41	112	5,400	76	120	645	78	435	20	120	90	195	270
K	0.28	5.5	12.4	3.4	1.6	155	3,600	220	32	895	195	500	26	300	240	250	410
L	0.14	3.3	19.5	4.6	2.4	1200	1,800	115	—	750	—	330	—	405	255	375	750
M	0.17	4.0	16.3	4.4	2.5	670	5,700	77	—	650	—	270	—	270	400	385	765
N	0.36	2.1	20.7	9.4	1.2	310	1,700	80	~37	1100	ND	805	13	740	115	150	685
GS 7202-35	0.030	0.29	25.2	9.5	3.7	725	3,700	86	—	1310	100	600	2.9	840	115	130	570

Note: For definition of groups A to N, see Table 3. The lowest line shows data for core GS 7202-35 (see also caption to Table 6 and Boström et al., 1974a). This table shows the normalized values from Table 4, obtained by the multiplication of the Ti, Al, Fe . . . , Zn values for each group  $i$  with a factor  $F_i$ , defined as follows:

$$F_i = \frac{40}{(4Al_i + Ti_i + Fe_i + Mn_i + P_2O_5_i + Ba_i)}$$

(all input data given in wt %). This expression is justified by the following facts: (a) In well-analyzed sediments with no opaline silica the sum of the oxides, hydroxides, and other compounds of Si, Al, Ti, Fe, Mn, P, and Ba constitute about 85% of the carbonate-free fraction or about half that amount (~40%) that concerns the sum of the elements Si, Al, Ti, etc. (b) In sediments with little or no opaline silica the ratio SiO<sub>2</sub>/Al<sub>2</sub>O<sub>3</sub> usually ranges between 3 and 4, the ratio found in average continental crustal matter (see Table 8); that is, the inorganic Si<sub>i</sub> ≈ 3 Al<sub>i</sub> in the sediments. In the expression for  $F_i$  above, 3 Al<sub>i</sub> thus stand for the inorganic Si fraction and 4 Al<sub>i</sub> thus for the combined Si<sub>i</sub> (inorg.) and Al<sub>i</sub> contributions. The best test of a method is to check whether it works or not. In carefully analyzed deep-sea sediments with much terrigenous matter Al usually ranges between 8%–9%, Fe usually between 4%–5%, and B between 110–135 ppm (Landergrén, 1964). These values compare well with respective values for groups E, H, and I, which show heavy admixture of terrigenous matter. A more detailed discussion of the need for sediment petrographic normalization procedures is presented in Boström et al., 1972b. However, the method tends to punish sediment data from active ridges; thus the average values for core GS7202-35 on the lowest line would be about 10% higher if a recalculation is made using obtained CaCO<sub>3</sub>, NaCl, KCl, MgCl<sub>2</sub>, and SrCO<sub>3</sub> concentrations.

TABLE 6  
Accumulation Rates for Constituents in Sediments Recovered During DSDP Leg 34

Group	SiO <sub>2</sub>	SiO <sub>2</sub> *	Ti	Al	Fe	Fe*	Mn	P <sub>2</sub> O <sub>5</sub>	Ba	B	Co	Cr	Cu	La	Ni	Sc	V	Y	Zr	Zn
<b>Hole 319</b>	(in mg/cm <sup>2</sup> 1000 yr)										(in mg/cm <sup>2</sup> 1,000,000 yr)									
A	9.6	3.5	0.053	0.83	4.4	3.9	1.3	0.69	0.30	5	7	0.4	28	9	18	0.6	6	40	24	26
B	16	8.5	0.086	0.95	8.7	8.1	1.9	0.83	0.55	9	8	0.5	55	10	24	0.6	15	23	14	22
C	61	24	0.32	5.0	88.0	85.0	34	8.6	3.1	180	58	<18	650	65	250	11	340	100	94	400
D	36	17	0.17	2.5	39.0	38.0	12	4.9	1.5	83	27	< 9	210	<18	97	< 3.6	110	34	36	130
<b>Hole 320</b>																				
E	168	-25	1.2	26	14.0	-1.6	0.56	0.50	1.1	38	6	26	83	9	73	5	71	8	40	110
F	47	26	0.15	2.8	23.0	21.0	0.67	1.3	1.0	39	10	?	130	?	39	?	48	11	25	77
G	9.2	6.8	0.025	0.32	5.6	5.4	1.9	0.41	0.19	15	2	?	31	?	16	?	20	3	5	17
<b>Site 321</b>																				
H	290	-13	2.0	41	27.0	2.4	0.35	0.97	1.9	58	27	47	290	24	97	8	97	24	92	110
I	116	12	0.74	14	10.0	1.6	0.21	0.50	1.0	23	11	19	120	13	71	3	22	15	38	44
J	54	4.4	0.34	6.7	6.4	2.4	0.42	0.41	0.53	11	8	12	63	8	43	2	12	9	19	26
K	48	0	0.32	6.5	15.0	11.0	4.0	1.9	0.42	18	27	4	110	23	59	3	35	29	30	49
L	14	1.4	0.014	1.7	9.9	8.9	2.4	1.2	0.09	62	6	< 8	38	< 8	17	< 2	21	13	19	38
M	40	7.4	0.18	4.4	18.0	15.0	4.8	2.7	0.62	73	8	<21	71	21	29	6	29	44	42	84
N	19	7.9	0.27	1.5	15.0	14.0	6.9	0.88	0.13	23	6	3	80	-	60	0.9	55	9	11	51
GS 7202-35	34	28	0.074	0.72	63.4	63.0	24	9.4	0.94	180	22	-	330	31	150	0.80	210	24	32	140

Note: Values for groups F and G may be too low. SiO<sub>2</sub>\* represents opaline silica, which is the quantity of SiO<sub>2</sub> that exceeds the value to be expected from the ratio SiO<sub>2</sub>/Al in continental matter (Table 8). Fe\* represents authigenic iron, which is the quantity of Fe that exceeds the value to be expected from the ratio Fe/Al in continental matter (Table 8). Negative values for Fe\* and SiO<sub>2</sub>\* implies losses due to weathering; characteristically these deficits occur in samples that are rich in terrigenous matter deposited close to the continents (groups E and H). In Hole 319 and Site 321 the deposits with the highest accumulation rates for Fe\* invariably occur in the basal part of the sediment column. The lowest line shows the accumulation rates in core GS 7202-35, which was obtained very close to the spreading center on the present East Pacific Rise. Position: 14°47.9'S, 113°30.1'W, depth 3044 m (corrected), total core length 8.5 m; for details, see Boström et al., 1974.

TABLE 7  
Average Accumulation Rates and Compositions of Sediments Rich  
in "Volcanic" Matter (I) and in Terrigenous Matter (II),  
Based on Material from DSDP Leg 34

	I <sup>a</sup>		II <sup>b</sup>	
	Average Accumulation Rate	Average Composition (CaCO <sub>3</sub> & NaCl Free)	Average Accumulation Rate	Average Composition (CaCO <sub>3</sub> & NaCl Free)
SiO <sub>2</sub>	30.5	23	157	57
SiO <sub>2</sub> *	12.1	8.5	19	6.8
Ti	0.18	0.14	1.1	0.39
Al	2.9	2.3	21.9	7.9
Fe	24.8	19.1	14.4	5.2
Fe*	23.1	17.8	1.2	0.43
Mn	8.4	6.5	0.39	0.14
P <sub>2</sub> O <sub>5</sub>	2.7	2.1	0.60	0.22
Ba	0.84	0.65	1.1	0.41
B	57	440	32	115
Co	18	140	13	47
Cu	155	1200	139	500
Ni	112	860	71	260
Sc	≈3.1	≈24	4.5	16
V	76	590	50	180
Y	37	285	14	50
Zr	35	270	47	169
Zn	100	770	73	260

Note: Data for the major constituents SiO<sub>2</sub> to Ba are given in mg/cm<sup>2</sup>1000 yr and wt %, respectively, and for the trace constituents B to Zr in mg/cm<sup>2</sup> 1,000,000 yr and wt ppm, respectively. The average compositions for the sediments are obtained from the average accumulation rates, using the assumption that the sum of the oxides, hydroxides, sulfates, and Ca compounds of the major constituents SiO<sub>2</sub>, Ti, Al, Fe, Mn, P<sub>2</sub>O<sub>5</sub>, and Ba constitute 85% of the CaCO<sub>3</sub>- and NaCl-free fraction of the sediments.

<sup>a</sup>The accumulation rates and composition of the basal sediments, rich in "volcanic" matter, are based on data in Table 6 for groups A, B, C, D, K, L, M, and N, that is, for sediments that were emplaced within 15 m.y. of the formation of the oceanic crust.

<sup>b</sup>The accumulation rates and composition of sediments rich in terrigenous matter are based on data in Table 6 for groups E, H, I, and J, that is, for sediments that were emplaced more than 15 m.y. after the formation of the oceanic crust.

in Figure 4. To some extent major constituents have to be discussed also in this section.

The basal sediments (group I of Table 7) are too rich in Fe, Mn, Ba, Cu, Ni, V, and Zn to be formed mainly from terrigenous matter (TM); see Figure 4a. Biological matter (BM) alone cannot explain their origin either, since BM has a distinctly different Al/Ti ratio and is too poor in Fe, Mn, V, and Zr (see Figure 4b). On the other hand, a sediment model consisting of 88% EPR matter (EPRD) and 12% TM gives a very good reproduction of the basal sediments (see Figure 4c). These proportions are well defined; already a shift to the proportions 3:1 for EPRD:TM gives a model sediment with distinctly poorer fit. Some addition (25%) of BM does not alter the situation much, but an admixture of 50% BM does give a poor fit (Figure 4d).

These findings, however, do not clarify the origin of the EPR constituents, which obviously are of importance when we discuss both the major and the trace element geochemistry of East Pacific sediments. Neither BM nor TM are sufficient sources of Mn, Fe, Ba, Ni, B, and Cu. Accumulation rate data for Al and Ti, both for these sediments and for the Pacific in general (Table 6, this paper, and Boström, in press) demonstrate that TM must be a totally insufficient source for most trace constituents, since TM is poor in trace constituents. BM, on the other hand, is fairly rich in trace elements relative to Al and Ti. One can therefore suspect that a mixture of BM and an unknown additional source (volcanic?) will give rise to EPRD as shown in Table 8. Figure 4e shows a possible solution to this problem. A consequence of this solution is that (compare Figures 4c and 4e) the

TABLE 8  
Compositions of Constituents in Model Sediments  
(in wt % on an Absolute Basis)

	BM <sup>a</sup>	TM <sup>b</sup>	VM <sup>c</sup>	EPRD <sup>d</sup>
SiO <sub>2</sub>	17.4	53.3	—	3.69
Al	0.28	8.1	—	0.083
Ti	0.037	0.48	—	0.0085
Fe	0.48	4.9	27	7.30
Mn	0.015	0.088	9	2.76
Ba	0.048	0.054	2.6	0.24
B	0.039	0.0078	—	0.021
Cu	0.028	0.0057	—	0.038
Ni	0.0093	0.0090	—	0.017
V	0.0020	0.013	0.050	0.025
Zn	0.089	0.0078	—	0.017
Zr	0.0025	0.019	—	0.0037
CaCO <sub>3</sub>	32.2	7.3	—	67

<sup>a</sup>BM: Composition of average dry marine biological matter, primarily plankton, based on a large number of analyses from the literature and laboratory work at RSMAS; for details, see Boström et al., 1974b and Moore et al., in preparation. The standard errors for most minor and trace constituents in biological matter is very small once the analyses have been normalized; for a detailed account, see Boström et al., 1974b.

<sup>b</sup>TM: Composition of terrigenous matter, derived from the assumption that weathered continental matter consists to 75% of average shale and to 25% of average continental crust. These proportions are obtained from the observation that the surface of the continents are to 75% covered by sedimentary deposits. Crust and shale abundances are from Krauskopf (1967).

<sup>c</sup>VM: See text. This hypothetical phase is identical to the one used in Boström, in press. The Ba-value is probably too high, but is difficult to estimate.

<sup>d</sup>EPRD: Composition of East Pacific Rise deposits, according to analyses of core GS 7202-35; similar values are reported for the Risepac cores 68 and 69. (Boström et al., 1974a; Boström and Peterson, 1969.)

basal sediments are formed by 44% BM, 44% "volcanic" matter (VM), and 12% TM. By using the same model inputs and calculations, one can find that the group II sediments (see Table 7) are produced by a mixture of about 74% BM, 24% TM, and 2% VM.

The origin of this "volcanic" phase is not clear. It appears likely, in view of their high accumulations rates, that Fe and Mn must be delivered in association with the plate generating volcanism at spreading centers; and Ba, Cu, and Ni, for instance, may be derived by absorption from seawater. It should be recalled, however, that elements which for quantitative reasons easily can be modeled as adsorbates, may nevertheless have a different source; this seems to be the case with U (Rydell et al., 1974). Furthermore, some "adsorption-explanations" may require very high removal efficiencies. Adsorption processes may indeed have been invoked too loosely in the past in view of the fact that quantitative removal by adsorption is difficult to achieve even in a laboratory where solution parameters

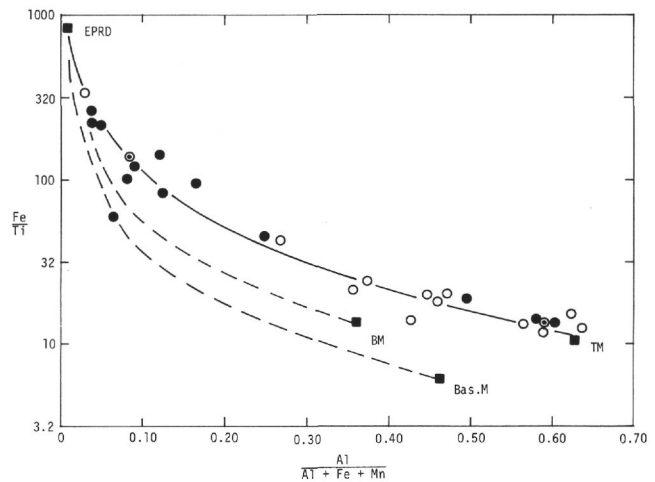


Figure 1. Relationships between  $Fe/Al$  versus  $Al/(Al + Fe + Mn)$ . Black dots represent data from this paper (Table 4), rings represent data for sediments from the open Pacific. (Each ring represents the average composition of sediments from one of several areas in the Pacific. Each of these averages is obtained using the average accumulation rates within each area; this procedure avoids the excessive weight that sediments from areas of slow deposition have; see Boström, in press.) Double rings represent averages for groups I and II; see Table 7 (data from this paper) and Boström, in press. The black square marked TM represents average terrigenous matter (see Table 8), and black square marked Bas.M represents average oceanic, tholeiitic basalt (see Manson, 1968). Black square BM represents average marine biological matter (see Table 8). It is obvious that mixing of average TM with average oceanic BM or average marine BM cannot explain much of the compositional variations in East Pacific sediments that concerns Al, Fe, Mn, and Ti. Mixing of average terrigenous matter with the extreme type of East Pacific Rise sediments such as GS 7202-35, black square marked EPRD, or Risepac 68, 69 (Boström and Peterson, 1969), on the other hand, gives an excellent fit between observed and predicted (solid curve) relations. This shows that almost all deep-sea sediments can be considered as mixtures of EPRD and TM with regard to the major constituents Al, Fe, Mn, and Ti. The figure further demonstrates that mixtures of basaltic matter with EPR sediments are virtually absent. These results are in excellent agreement with previously observed  $Fe/Ti-Al/(Al + Fe + Mn)$  relations (Boström, 1970; Boström et al., 1972b; 1973b). Furthermore, note that the EPR-matter has a fairly constant composition with a very high  $Fe/Al$  ratio; otherwise, it would be difficult to explain how almost all analyses (out of many hundred) of unconsolidated, nonconcretionary deep-sea sediments with a worldwide distribution fall on or very close to the mixing curve EPRD-TM, both according to data in this paper and in previous reports (Boström, 1970; Boström et al., 1972b). Furthermore, it is of interest to note that as analytical data have improved, the points tend to fall closer to this mixing curve, not scatter farther away from it.

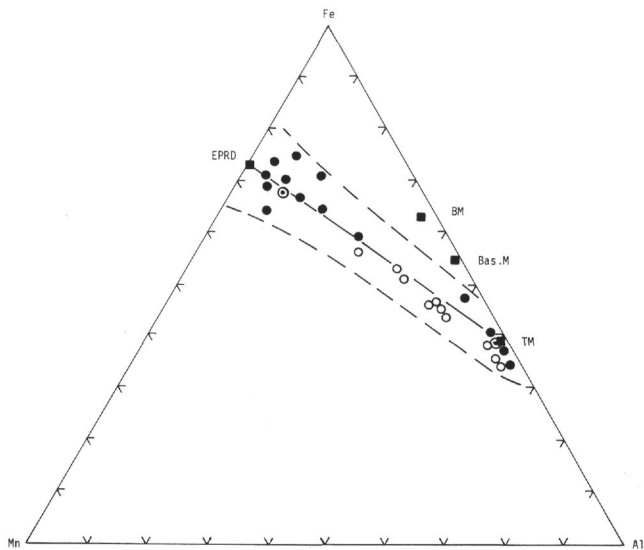


Figure 2. Relationships between Fe, Mn, and Al in East Pacific and pelagic sediments in general. Symbols are the same as in Figure 1. Note that all sediment averages from this and other works (Boström, in press) fall along the tieline between EPRD and TM, whereas there is no tendency for the points to cluster along the corresponding tielines (not shown) for EPRD-BM or EPRD-Bas.M. This suggests that biological matter and basaltic detritus, etc play a negligible role in the element budgets for Fe, Mn, and Al in the deep sea. (This does not mean that there are no sediments with heavy admixture of basaltic material, for instance, but that such mixtures are of local significance only, as is well demonstrated by the fact that basaltic components only show up in sediments that accumulate exceedingly slowly, as was shown by Boström et al., 1973b). Note that the relationships in this figure only pertain to unconsolidated, nonconcretionary sediments.

like pH can be optimized. Note, furthermore, that the model in Figure 4e shows a deficit in Ni and Cu, that cannot be resolved by the addition of more BM or TM; this will disrupt the major element relationships (see Figure 4f). The best explanation, therefore, appears to be that VM is indeed rich in Cu and Ni; in other words, VM approaches EPRD in composition. It cannot be ruled out at present that the bulk quantity of the EPRD, including its trace content, may have a volcanic source.

### General Geochemical Relationships

A final comment regarding the sediment models above is of interest. Thus, although the quantitative relationships for 10-13 constituents are involved, only two to three input phases are required in the models as demonstrated in Figures 4a to 4f. Deep-sea sediments far from spreading centers (which are the bulk of all deep-sea sediments) can usually be described with only two inputs, namely BM and TM (Boström et al., 1974b; Boström, in press; Moore et al., in preparation). This suggests that deep-sea sedimentation can, as a first-order approximation, be considered to be a simpler geochemical process than previously believed. It also implies that mixing of solid phases with fairly constant

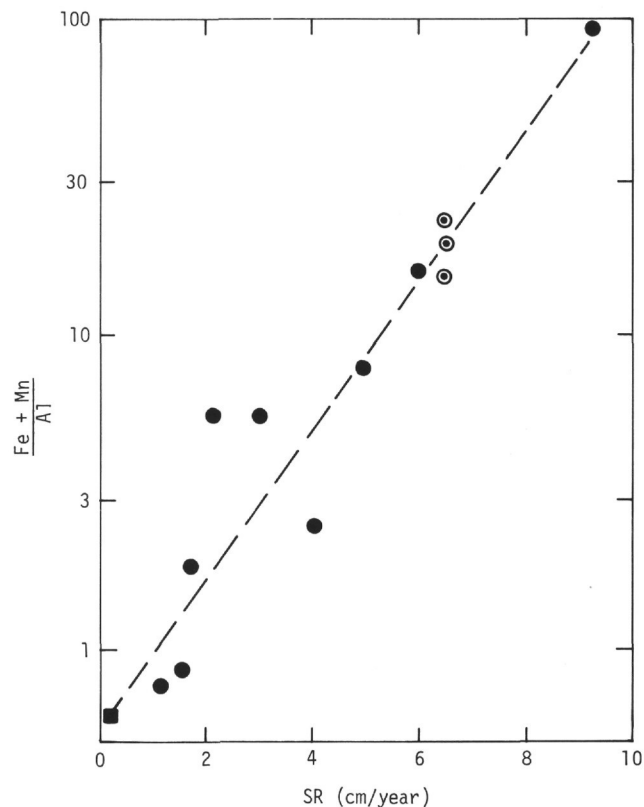


Figure 3. Relationship between crustal spreading rate (SR)

and the ratio  $\frac{\text{Fe} + \text{Mn}}{\text{Al}}$ . Solid circles represent data from

Boström (1973); circled dots the basal layers D, G, and N (this work), and squares the TM (Table 8) which is deposited in large quantities in areas of no spreading close to the oceans. The early set of data (solid circles) has a correlation coefficient of 0.93; for all the points in this graph, the correlation has improved to 0.96. Both of these correlation coefficients are well above the value for the 1% significance level.

compositions plays a much larger role than does transport of dissolved phases for the chemical composition of deep-sea sediments.

In this context it is of particular interest to note the behavior of EPRD in the graphs in Figures 1, 2, and 4 which suggests that the volcanic emanations must hydrolyze almost immediately after they surface on the ocean floor; otherwise one would expect much stronger tendencies for Fe, Mn, etc to segregate than is observed in the active ridge deposits. This implies that dissolved phases (except in the zone of emanations) play subordinate roles in the formation of deep-sea sediments, possibly with the exception for Mn and Ba. Other exceptions are, of course, Na, K, Ca, and Sr, which are present in seawater in high concentrations.

### Special Problems

#### Geochemistry of Ba

The geochemistry of Ba is perhaps more incompletely known than that of other elements. Association with

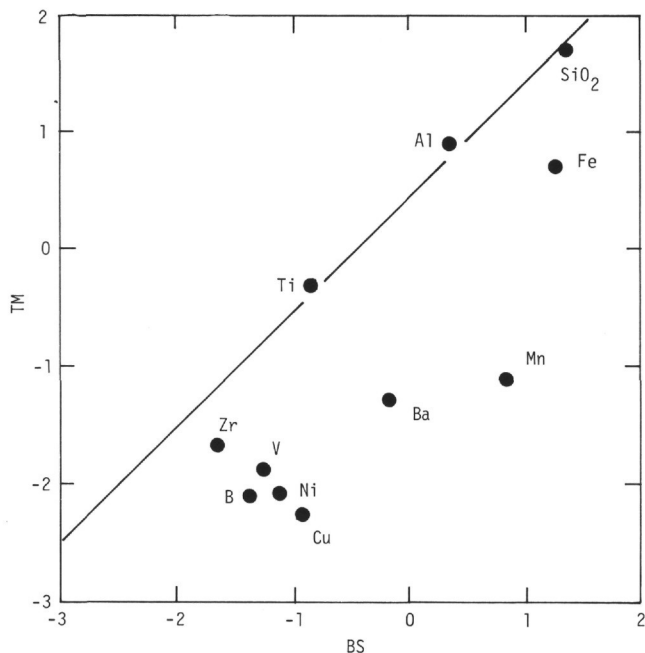


Figure 4a. Geochemical graphs, showing the relationships between the composition of the sediment sources and the sediments in the East Pacific sampled during Leg 34. All values represent the logarithm for the concentration given in %. Input constituents are from Table 8, in which BM stands for biological matter, TM stands for terrigenous matter, VM stands for volcanic matter (of hypothetical nature), and EPRD stands for East Pacific Rise Deposits as recovered at site GS 7202-35 (see Tables, 6 and 8). Geochemical models of this type have been extensively used and described in Boström et al., 1974a; Boström, in press; Moore et al., in preparation. (a) Relations between TM and average basal sediments (BS) as given in Table 7.

biological processes is obvious, but strong ties with volcanic processes are also evident (Arrhenius and Bonatti, 1965; Bonatti et al., 1972; and Boström et al., 1973a). It is characteristic that modeling for most constituents in the graphs presented in Figure 4a of this work and in Boström et al. (1974b), is fairly easy. Ba, however, has presented persistent difficulties, that we do not fully understand. It is obvious that our knowledge of how much Ba is present in BM, TM, and basaltic matter must be wrong, or that Ba has a migration tendency similar to Mn (Lynn and Bonatti, 1965; Bonatti et al., 1971; Boström and Fischer, 1972).

#### Geochemistry of Sc and Zr

The discussion above gives a somewhat erroneous impression of the geochemistry of Zr and Sc. Thus, Table 7 suggests that the basal layer is richer in these constituents than are the overlying deposits. A more careful study of Table 5 reveals, however, that the lowermost part of the basal section (which generally is the one with the fastest accumulation) shows fairly low concentrations of these elements, as was earlier indicated by studies of recently formed deposits, resting almost

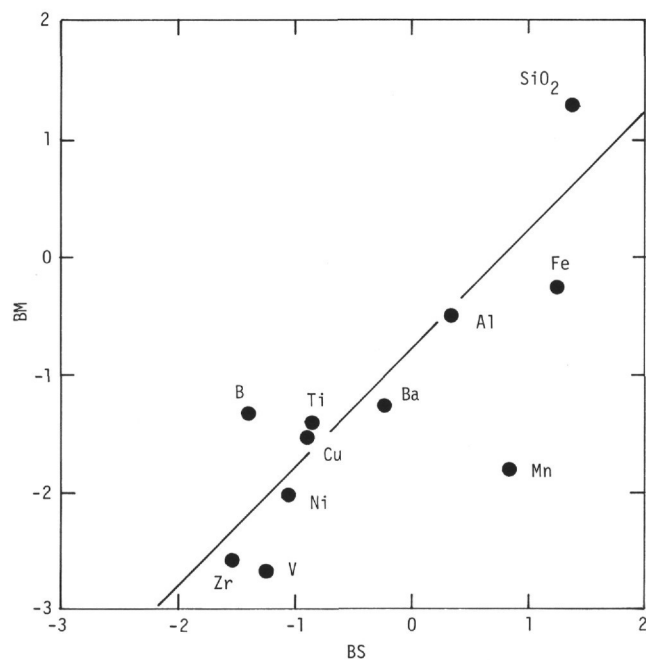


Figure 4b. Relationships between BM and average basal sediments as given in Table 7. In both (a) and (b) the fit is very poor. In these and the following diagrams the diagonal line represents the best fit to the most important hydrolysates Al and Ti; their immobility make them excellent markers of the extent a sediment model can satisfactorily explain the composition of a given sediment. Too little Mn, Fe, and V are supplied to models (a) and (b) to explain the origin of the basal sediments in the East Pacific with TM or BM alone.

directly on the basalt substratum. A more proper breakdown of the sediments might therefore have been to divide them in three major layers, of which layer 2, forming far from both spreading centers and from the continents, would show the strongest incorporation of adsorbates and biogenic matter.

#### Bauer Deep Deposits

The Bauer Deep deposits have received particularly great attention due to their strange appearance. Boström and Peterson (1966, 1969) reported not only very high concentrations of Fe and Mn, as were known from Revelle's (1944) work, but also very high concentrations of Cu, Ni, and Co; subsequent studies also have shown very high concentrations of Zr, Sc, Ba, and rare earths in these sediments (Boström et al., 1972a, 1973a; Boström, 1973). Similar results as well as very thorough mineralogical studies of the same sediments were reported by Sayles and Bischoff (1973). An extensive discussion of the relationship between heat flow and metallogenesis in the Bauer Deep was presented by Anderson and Halunen (1974).

The findings in this paper do not contradict these experimental results, but perhaps do contradict some earlier conclusions regarding the origin of these sediments. Data in Table 6 suggest that groups A and B at Site 319 (which is representative of present-day sedi-

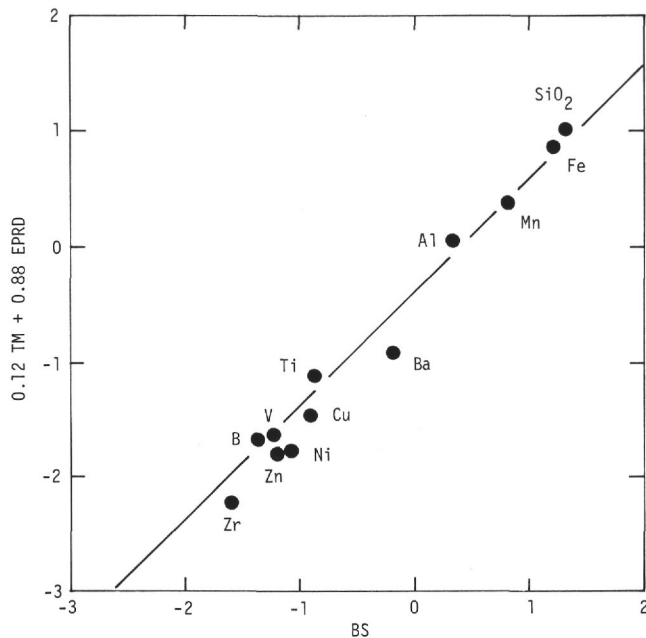


Figure 4c. Relationships between a mixture of 12% TM + 88% EPRD versus average basal sediments. The fit is good, suggesting that not only major constituents (as in Figures 1 and 2) can be explained by mixing of TM and EPRD, but also the abundance of the trace elements.

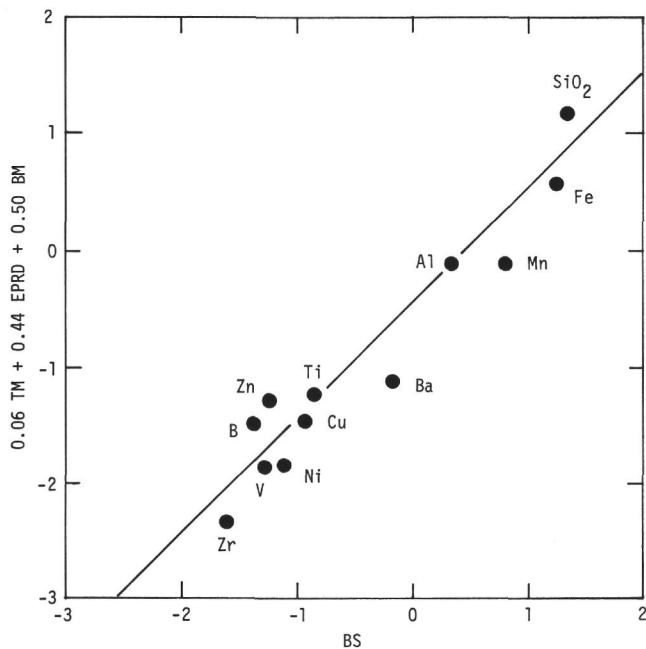


Figure 4d. The model in (c) can be admixed with some BM, but not very much. Already an admixture of 50% as in this graph gives a poorer fit than in (c). At most, 25% BM can be admixed without ruining the fit in (c).

mentation conditions in the Bauer Deep) have no unusually high accumulation rates of any constituent; on the contrary, it is a basin with exceedingly sluggish deposition rates at present. This means that adsorption processes, later alterations, hydrothermal "washing" of the sediments, etc will have much time available to leave

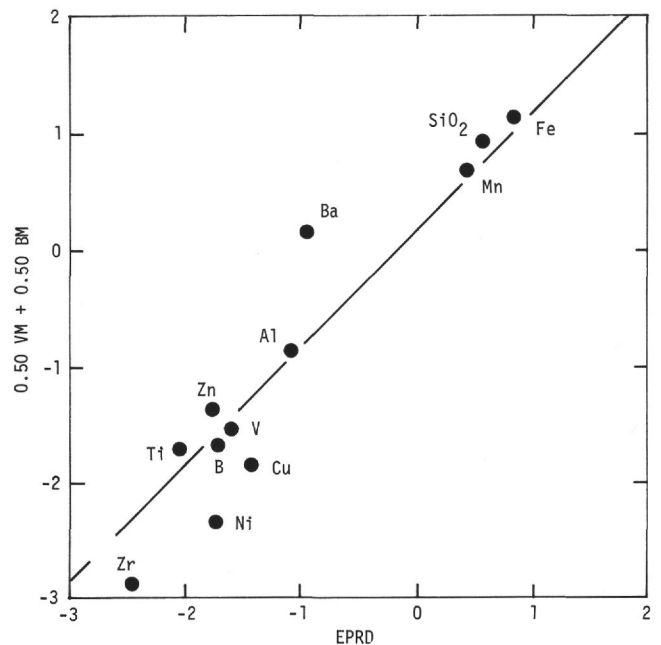


Figure 4e. Model showing how EPRD possibly can be explained as due to mixture of VM and BM in the proportions 1:1. The fit is not very good, however.

their geochemical imprint on these sediments. To use these sediments as particularly useful indicators of what is going on during metallogenesis, as suggested by Anderson and Halunen (1974), is therefore risky. This conclusion is supported by data for groups C and D from Hole 319 (see Tables 5 and 6); the former table shows much lower values for Ba, Co, La(?), Y, and Zr; a decreasing trend may also be present for Ni and Sc. Note that groups A to D fall almost exactly on the mixing curve EPRD-TM in Figure 1.

The conclusion from these findings is that the Bauer Deep is the worst area to study if we want to understand the origin of rapidly forming active ridge deposits. Due to the slow admixture rate of both the typical active ridge sediments as we know them from the crest of the EPR (for instance, GS 7202-35) and of terrigenous matter, the present-day Bauer Deep deposition is exceedingly sensitive to other processes, including trace element or isotope input from other sources. Such studies should be performed on typical active ridge sediments, which accumulate much faster than those in the Bauer Deep.

An additional interesting conclusion can be obtained from the data presented in this paper and in Anderson and Halunen (1974). The very fact that the pronounced heat-flow anomaly in the Bauer Deep (Anderson and Halunen, 1974) has caused such insignificant accumulation rates for the constituents Fe, Mn, etc., throws severe doubts over the prevailing interpretation that heat flow-induced seawater leaching of the oceanic crust accounts for the origin of the major fraction of the active ridge deposits. This is in good agreement with the findings by Rydell et al. (1974), who conclude that additional sources of a more deep-seated nature are needed to explain the composition of active ridge deposits.

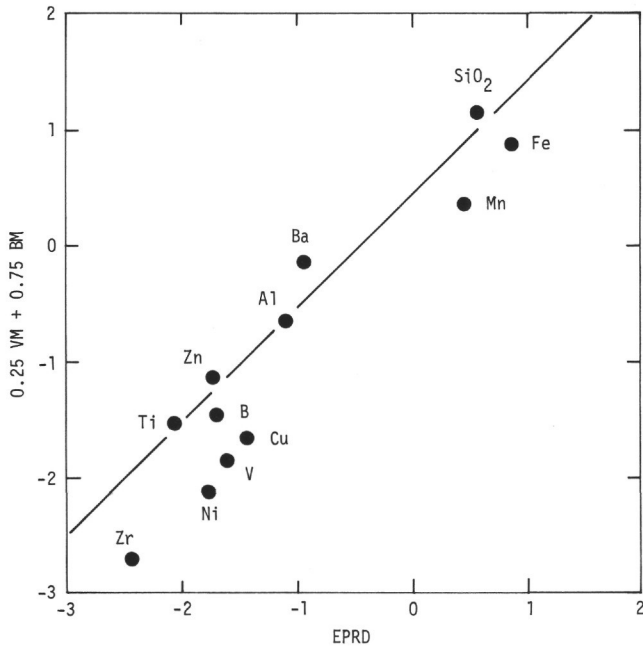


Figure 4f. In the previous model (e) Cu, Ni, and Zr values were too low to fit the model well. Additional BM will not improve the situation, as this graph with 1 part VM and 3 parts BM shows; the fit for Fe, Mn, B, and V is lost and the fit for Cu and Ni has not appreciably improved. This may indicate that a volcanic phase with abundant Fe, Mn, V, and Ba as well as many trace elements such as Cu and Ni must be resorted to, that is, the hypothetical VM in Table 8 should approach EPRD in composition.

### CONCLUSIONS

1. Sediments from DSDP Leg 34, which traversed one flank of an active ridge (EPR), show remarkable similarities with those obtained from the spreading ridge in the South Atlantic during DSDP Leg 3. Thus, the basal sediments are rich in Fe, Mn, and V, and poor in Al, Ti, and Si. The formation of these basal sediments was completed within about 15 m.y. or less after the generation of the basaltic crust on which the sediments rest.

2. Analyses of chemical data reveal that the basal sediments can be considered to have formed from two components: one a volcanic phase, very similar to the inorganic fraction presently being deposited on the crest of the EPR (but probably with some admixed biogenous matter); and the second, a terrigenous phase.

3. Accumulation rates for characteristic constituents in this volcanic phase (authigenic Fe, Mn, V) are very high, often up to 10-100 times the values found for deposits formed far from spreading centers.

4. Seawater leaching of basaltic rock is an unlikely source for the volcanic emanations deposited in the basal sediments; otherwise one would expect the present-day heat-flow anomalies in the Bauer Deep to be associated with much higher accumulation rates for Fe, Mn, etc than is now the case. No experimental leaching experiments involving basalt and NaCl brines

have produced the Al-Fe separation that is required to explain the composition of active ridge deposits, nor do observations of hot spring waters in basaltic terranes show such separations. These facts contradict the seawater leaching hypothesis.

5. As has been pointed out elsewhere, carbonate-rich emanations of deep-seated origin are the most likely source for the anomalously Fe-Mn-rich active ridge deposits, as well as for much of their content of Ba, P, and U. Such a source could also explain why active ridge deposits are so persistently poor in Si, Al, Ti, and Th compared to other deep-sea sediments.

6. Studies of sediment models suggest that the volcanic emanations hydrolyze immediately after they surface, and that they subsequently, in a particulate form, are admixed with terrigenous and biogenous matter in various proportions. This implies that outside the emanation zone, dissolved matter and solutions play but a small role in the origin of deep-sea sediments, an interpretation that is supported by the data in Figures 1, 2, and 4.

### ACKNOWLEDGMENTS

This research was supported by the National Science Foundation Grant NSF-GX-40428. This is a contribution from the Rosenstiel School of Marine and Atmospheric Sciences and from the Department of Economic Geology, University of Lulea.

### REFERENCES

- Anderson, R.N. and Halunen, A.J., 1974. Implications of heat flow for metallogenesis in the Bauer Deep: *Nature* v. 251, p. 473-475.
- Arrhenius, G.O.S. and Bonatti, E. 1965. Neptunism and volcanism in the ocean. In Sears, M. (Ed.), *Progress in oceanography*, Volume 3: Washington (Am. Assoc. Adv. Sci.), p. 7-22.
- Barth, T.F.W., 1952. *Theoretical petrology*: New York (John Wiley & Sons).
- Berggren, W.A., 1969. Rates of evolution in some Cenozoic planktonic foraminifera: *Micropaleontology*, v. 15, p. 351-365.
- Bonatti, E., Fisher, D.E., Joensuu, O., and Rydell, H.S., 1971. Postdepositional mobility of some transition elements, phosphorous, uranium, and thorium in deep-sea sediments: *Geochim. Cosmochim. Acta*, v. 35, p. 189-201.
- Bonatti, E., Fisher, D.E., Joensuu, O., Rydell, H., and Beyth, M., 1972. Iron-manganese-barium deposit from the Northern Afar rift (Ethiopia): *Econ. Geol.*, v. 67, p. 717-730.
- Boström, K., 1967. The problem of excess manganese in pelagic sediments. In Abelson, P.M. (Ed.), *Researches in geochemistry*, Volume 2: New York (John Wiley & Sons), p. 421-452.
- \_\_\_\_\_, 1970. Submarine volcanism as a source for iron: *Earth Planet. Sci. Lett.*, v. 9, p. 348-354.
- \_\_\_\_\_, 1973. The origin and fate of ferromanganoan active ridge sediments: *Acta Univ. Stockholmiensis, Stockholm Contrib. Geol.* v. 27, p. 149-243.
- \_\_\_\_\_, in press. Particulate and dissolved matter as sources for pelagic sediments: *Acta Univ. Stockholmiensis, Stockholm Contrib. Geol.*
- Boström, K. and Fisher, D.E., 1972. Lateral fluctuations in pelagic sedimentation during the Pleistocene glaciations: *Boreas*, v. 1, p. 275-288.

- Boström, K., and Peterson, M.N.A., 1966. Precipitates from hydrothermal exhalations on the East Pacific Rise: *Econ Geol.*, v. 61, p. 1258-1265.
- , 1969. Origin of aluminum-poor ferromanganoan sediments in areas of high heat flow on the East Pacific Rise: *Marine Geol.*, v. 7, p. 427-447.
- Boström, K., Farquharson, B., and Eyl, W., 1972a. Submarine hot springs as a source of active ridge sediments: *Chem. Geol.*, v. 10, p. 189-203.
- Boström, K., Joensuu, O., Valdés, S., and Riera, M., 1972b. Geochemical history of South Atlantic Ocean sediments since late Cretaceous: *Marine Geol.*, v. 12, p. 85-121.
- Boström, K., Joensuu, O., Moore, C., Boström, B., Dalziel, M., and Horowitz, A., 1973a. Geochemistry of Ba in pelagic sediments: *Lithos*, v. 6, p. 159-174.
- Boström, K., Kraemer, T., and Gartner, S., 1973b. Provenance and accumulation rates of opaline silica, Al, Ti, Fe, Mn, Cu, Ni and Co in Pacific pelagic sediments: *Chem Geol.*, v. 11, p. 123-148.
- Boström, K., Joensuu, O., Kraemer, T., Rydell, H., Valdés, S., Gartner, S., and Taylor, G., 1974a. New finds of exhalative deposits on the East Pacific Rise: *Geol. Fören. Stockh. Förhandl.*, v. 96, p. 53-60.
- Boström, K., Joensuu, O., and Brohm, I., 1974b. Plankton—its chemical composition and its significance as a source of pelagic sediments. *Chem. Geol.*, v. 14, p. 255-271.
- Corliss, J.B., 1971. The origin of metal-bearing submarine hydrothermal solutions: *J. Geophys. Res.*, v. 76, p. 8128-8138.
- Green, H.W., II, 1972. A CO<sub>2</sub> charged asthenosphere: *Nature, Phys. Sci.*, v. 238, p. 2-5.
- Hays, J.D., Cook, H., Jenkins, G., Orr, W., Goll, R., Cook, F., Milow, D., and Fuller, J., 1972. An interpretation of the geologic history of the Eastern Equatorial Pacific from the drilling results of *Glomar Challenger*, Leg 9. In Hays, J.D. et al., 1972. Initial Reports of the Deep Sea Drilling Project, Volume 9: Washington (U.S. Government Printing Office), p. 909-931.
- Herron, E.M., 1972. Sea-floor spreading and Cenozoic history of the East Central Pacific: *Geol. Soc. Am. Bull.*, v. 83, p. 1671-1692.
- Krauskopf, K.B., 1967. Introduction to geochemistry: New York (McGraw-Hill).
- Landergren, S., 1964. On the geochemistry of deep sea sediments. Rept. Swedish Deep Sea Exped., v. 5, p. 1-154.
- Lynn, D.C. and Bonatti, E., 1965. Mobility of manganese in diagenesis of deep-sea sediments: *Marine Geol.*, v. 3, p. 457-474.
- Manson, V., 1968. Geochemistry of basaltic rocks: major elements. In Hess, H.H. and Poldervaart, A., (Eds.), *Basalts*: New York (John Wiley & Sons), v. 1, p. 215-269.
- Moore, C. and Boström, K., in preparation. Lower marine organisms: their geochemistry and role as a source for trace elements in deep sea deposits.
- Revelle, R.R., 1944. Marine bottom samples collected in the Pacific by the Carnegie on its seventh cruise: Washington (Carnegie Inst. Wash.), Publ. 556.
- Rydell, H., Kraemer, T., Boström, K., and Joensuu, O., 1974. Postdepositional injections of U-rich solutions into East Pacific Rise sediments: *Marine Geol.*, v. 17, p. 151-164.
- Sayles, F.L. and Bischoff, J.L., 1973. Ferromanganoan sediments in the Equatorial East Pacific: *Earth Planet. Sci. Lett.*, v. 19, p. 330-336.
- Sillitoe, R.H., 1972. Relations of metal provinces in Western America to subduction of oceanic lithosphere: *Geol. Soc. Am. Bull.*, v. 83, p. 813-818.
- Turekian, K.K., 1968. Deep-sea deposition of barium, cobalt and silver: *Geochim. Cosmochim. Acta*, v. 32, p. 603-612.
- van Andel, T.J.H., Corliss, J.B., and Bowen, V.T., 1967. The intersection between the Mid-Atlantic Ridge and the Vema Fracture Zone in the North Atlantic: *J. Mar. Res.; Sears Found. Mar. Res.*, v. 25, p. 343-351.